Storage and balancing synergies in a fully or highly renewable pan-European power system

Morten Grud Rasmussen[a,b,1], Gorm Bruun Andresen[b,2], Martin Greiner[b]

[a] *Center for Mathematical Sciences and Institute for Advanced Study, Technische Universität München, 85748 Garching, Germany*
[b] *Department of Engineering and Department of Mathematics, Aarhus University, Ny Munkegade 118, 8000 Aarhus C, Denmark*

Abstract

Through a parametric time-series analysis of eight years of hourly data, we quantify the storage size and balancing energy needs for highly and fully renewable European power systems for different levels and mixes of wind and solar energy. By applying a dispatch strategy that minimizes the balancing energy needs for a given storage size, the interplay between storage and balancing is quantified, providing a hard upper limit on their synergy. An efficient but relatively small storage reduces balancing energy needs significantly due to its influence on intra-day mismatches. Furthermore, we show that combined with a low-efficiency hydrogen storage and a level of balancing equal to what is today provided by storage lakes, it is sufficient to meet the European electricity demand in a fully renewable power system where the average power generation from combined wind and solar exceeds the demand by only a few percent.

Keywords: energy system design, wind power generation, solar power generation, large-scale integration, storage

1. Introduction

A fully renewable pan-European power system will depend on a large share of non-dispatchable, weather dependent sources, primarily wind and solar power

Email address: mgr@imf.au.dk (Morten Grud Rasmussen)
[1]This author is supported by Carlsbergfondet
[2]This author is supported by DONG Energy

(Czisch (2005); Jacobson and Delucchi (2011)). The optimal ratio between and necessary amount of wind and solar power depends on storage and balancing resources (Heide et al. (2010, 2011); Hedegaard and Meibom (2012)), transmission (Czisch and Giebel (2007); Kempton et al. (2010); Schaber et al. (2012a,b)), and the characteristics of the climate (Widén (2011); Aboumahboub et al. (2010)) and load (Yao and Steemers (2005)). Based on meteorological data, it was shown that even with unlimited transmission within Europe, a scenario with only wind and solar power in combination with either only storage (Heide et al. (2010)) or only balancing (Heide et al. (2011)) requires a very large amount of excess generation in order to be technically feasible. Here, we study the intermediate and more realistic scenarios where power generation from the two weather-driven variable renewable energy (VRE) sources is backed up by specific combinations of storage and balancing. We identify a class of realistic and feasible scenarios for building a fully or partially renewable pan-European power system.

The main point of our paper is to outline what is possible in a wind and solar based European power system with storage and balancing systems. The power capacities of the storage and balancing facilities are not determined; this would require a more complex modeling with explicit inclusion of power transmission (Rodriguez et al. (2012)). We focus on wind and solar power and assume no bottlenecks in the power grid, employ an optimal storage dispatch strategy and ignore storage charge and discharge capacities and economic aspects. The incentives for doing so are closely related and at least threefold.

By assuming few technical constraints and optimal operation strategy, our results provide a hard upper limit on what can be accomplished by better intercontinental power network integration, better technology or better market design. This means that more realistic models have a solid frame of reference to be measured up against. At the same time, our results provide precise boundaries for policy makers. Furthermore, it allows for a simpler analysis and a clearer presentation. The price is that a more detailed model is necessary

in order to give useful answers to questions regarding e.g. charge, discharge[3], balancing or power flow capacities, and hence any considerations regarding the economic costs obviously become highly speculative within the current modeling framework.

A somewhat related but in some respects also parallel argument is behind the decision of focusing on wind and solar power. Three of the most scalable renewable energy sources are wind and solar power and biomass. Of these, biomass stands out as being *dispatchable*, meaning that it can be used for balancing the intermittent (or non-dispatchable) power sources, such as wind and solar power. As such, biomass is implicitly included in our analysis. Besides wind and solar power, one of the most important non-dispatchable power sources is run-of-river hydro power. Although run-of-river contributes significantly to the present-day power systems of Europe with some percent of the total generation, the perspective for future growth is highly limited (Lehner et al. (2005)), leaving it ill-suited as a third component in our parametric analysis. However, with available data, it would have been straight-forward and an obvious choice to include it as a fixed (but time dependent) contribution.

Contrary to most work done in this field (Czisch (2005); Jacobson and Delucchi (2011); Martinot et al. (2007); Lund and Mathiesen (2009)), the novel weather-based modeling approach, used here and first introduced in Heide et al. (2010), is designed to investigate a whole class of scenarios. This means that we do not only provide results for a few end-points, or for a pathway to any such. Rather, we provide a continuous *map* of results for any combination and penetration level of wind and solar power generation (Heide et al. (2010, 2011); Schaber et al. (2012b)). We do not attempt to show that a transition to a fully renewable power system is economically viable, however, this has been addressed by others (Czisch (2005); ECF (2010)). An advantage of disregarding the economical aspect is that our work is less sensitive to technological advances and socio-economic changes that could potentially shift the economic balance

[3]See, however, the Appendix

between e.g. wind and solar power.

The paper is organized as follows: Section 2 describes data and methodology. Section 3 briefly discusses the extreme scenarios of no storage and sufficiently large storage, respectively. Section 4 deals with the interplay between storage and balancing. Section 5 treats the concrete example of having a 6-hour storage. Section 6 discusses the impact of hydro balancing and large hydrogen storages. Finally, an appendix discusses storage operation strategies.

2. Data and methodology

2.1. Weather and load data

Historical weather data from the 8-year period 2000–2007 with a tempo-spatial resolution of 1 hour $\times$ 50 $\times$ 50 km^2 was used to derive wind and solar power generation time series for Europe (see Heide et al. (2010)). The data set comprise two 70128-hour long time series for each of the approximately 2600 grid cells, covering 27 European countries including off-shore regions. In this study all grid cells are aggregated using a capacity layout based on political goals and attractiveness of the sites (see Heide et al. (2010)). We thus have two hourly power generation time series for Europe, $w(t)$ for wind and $s(t)$ for solar power generation, where t denotes any hour of the 8-year period.

The electrical load time series $L(t)$ is based on data from the transmission system operators (TSO) for the same eight years. The load data was de-trended to compensate for the approximately 2% yearly increase in demand and scaled to 2007 values, where the total annual consumption amounted to 3240 TWh for Europe. This corresponds to an average hourly load (av.h.l.) of 370 GWh.

The power generation time series $w(t)$ and $s(t)$ have been normalized to the average electrical load, yielding two new time series, $W(t)$ and $S(t)$. As everything is scaled to 2007 values, we use the units av.h.l. (average hourly load) and av.y.l. (average yearly load) throughout the paper. This means that

$$W(t) = \frac{w(t)}{\langle w \rangle} \cdot \text{av.h.l.}, \quad S(t) = \frac{s(t)}{\langle s \rangle} \cdot \text{av.h.l.}$$

and

$$\langle L \rangle = \langle W \rangle = \langle S \rangle = 1 \,\text{av.h.l.},$$

where $\langle \cdot \rangle$ denotes the average value of a time series. In these units, the values of $L(t)$ all lie in the range 0.62–1.47 av.h.l. while $W(t)$ and $S(t)$ fall in the intervals 0.07–2.61 and 0.00–4.10 av.h.l., respectively. Figure 1 shows an excerpt of the time series.

2.2. Generation–load mismatch

The generation–load mismatch time series $\Delta(t)$ is given by

$$\Delta(t) = \gamma \cdot (\alpha_W \cdot W(t) + (1 - \alpha_W) \cdot S(t)) - L(t) \,, \tag{1}$$

where α_W denotes the wind power fraction of the average wind and solar power generation and γ represents how much combined wind and solar power is generated on average, so that if e.g. $\gamma = 1.00$, the average total generation of wind and solar power equals the average load. Using the standard notation

$$x_- = \begin{cases} 0 & \text{for } x \geq 0 \\ -x & \text{for } x < 0 \end{cases}, \quad x_+ = \begin{cases} x & \text{for } x \geq 0 \\ 0 & \text{for } x < 0 \,, \end{cases} \tag{2}$$

this means that $\Delta_-(t)$ denotes the residual load, and $\Delta_+(t)$ denotes possible excess generation. We will use the term *mix* for any fixed choice of α_W while γ is referred to as the *average VRE*[4] *generation factor*. An excerpt of the mismatch time series $\Delta(t)$ for an average VRE generation factor $\gamma = 1.00$ and a mix of $\alpha_W = 0.60$ together with the corresponding excerpt of the load and wind and solar power time series can be seen in Figure 1.

2.3. Balancing

As our focus is on wind and solar based, fully renewable power systems, we consider any dispatchable, additional power source to be balancing (excluding

[4] variable renewable energy

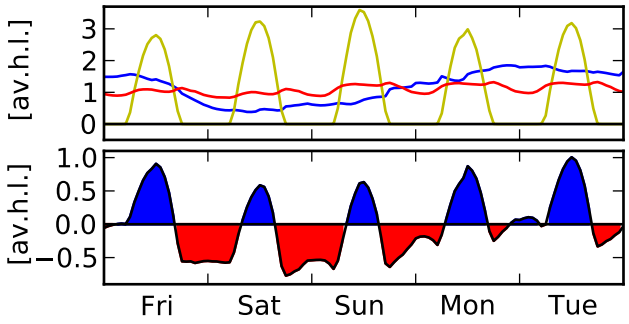

Figure 1: Top panel shows excerpts of the L(t) (red), W(t) (blue) and S(t) (yellow) time series, representing load and wind and solar power, respectively. Lower panel shows mismatch time series $\Delta(t)$ for the same days (black), with $\gamma = 1.00$ and $\alpha_W = 0.60$. The blue areas indicate excess generation, while the red indicate the residual load. The excerpt covers the time period 10–15 March 2000

storage). Thus, when no storage is present, the balancing time series is simply the residual load, or minus the negative values of $\Delta(t)$:

$$B(t) = \Delta_-(t) \qquad \text{(no storage)}, \tag{3}$$

corresponding to the red areas in the lower panel of Figure 1. In this paper, we will mainly focus on one property of the balancing time series, namely its average value (which we divide by the average load to get a dimensionless parameter):

$$E_B = \langle B \rangle / \langle L \rangle$$

E_B measures the share of the energy that must be provided by non-VRE resources to cover the demand. This means that one would hope for $E_B + \gamma = 1$ for $\gamma \leq 1$ and $E_B = 0$ for $\gamma > 1$, which can be rewritten as:

$$E_B = (1 - \gamma)_+, \tag{4}$$

because otherwise, more energy is put into the system[5] than is demanded. This also means that, with a perfect storage, or with perfect demand side management, (4) would hold (in fact, this could be the definition of being perfect).

[5] This would of course lead to curtailment

Unfortunately, (4) cannot be expected to hold. This means that, for a given γ, we could have $E_B > (1-\gamma)_+$, meaning that on average, we need additional balancing. This leads us to define the *additional average balancing* E_B^{add} as:

$$E_B^{\text{add}} = E_B - (1-\gamma)_+ \, .$$

One can think of E_B^{add} as a measure of how well the VRE resources can be integrated into the power system, or how much energy one on average would need to move in time to get perfect integration. We stress that E_B^{add} is a property that has to do with an *average* – it is not a priori possible to assign a time series to the additional balancing. As one always – given γ – can find E_B from E_B^{add} by adding $(1-\gamma)_+$, and because E_B^{add} makes some of the definitions related to storages easier, we will mainly use E_B^{add} rather than E_B, except when we deal with lossy storages, as the concept of additional balancing in this case becomes more complicated.

2.4. Storage

With our goal of outlining the borders of what is possible in a European power system with storage and balancing, in particular with respect to balancing energy E_B, we will focus on a storage dispatch strategy which, for a given storage size C_S, performs optimal with respect to E_B. This means that given a storage size, no storage dispatch strategy can result in a lower average balancing energy E_B than the one employed here. There are several strategies that satisfy this condition, meaning that they all result in the same E_B.

Here, we will present a version which has the advantages that it is simple and hence easily defined and is easily seen to satisfy the condition, and it assumes no foresight capabilities, but has the disadvantage that it is quite far from how present-day real-world operation works. Three other versions satisfying the minimum E_B condition are presented in the appendix.

The version presented here can be summed up as a "storage first" strategy, in the sense that any deficits are first covered with storage unless it runs empty, and any excess generation is stored in the storage, unless the storage gets full.

No limits are imposed on the charge and discharge capacities. Conversion losses in and out of the storage are modeled by storage efficiencies η_{in} and η_{out}. For example, for hydrogen storage, the efficiencies are approximately 0.60 in both directions (Beaudin et al. (2010); Kruse et al. (2002)), leading to a round-trip efficiency of 0.36.

A storage is thus characterized by three parameters: $\eta_{\text{in}}, \eta_{\text{out}}$ and C_S. The storage filling level time series $H(t)$ with a constrained storage size C_S is given by:

$$H(t) = \begin{cases} C_S & \text{for} \quad H(t-1) + \tilde{\Delta}(t) > C_S \ , \\ 0 & \text{for} \quad H(t-1) + \tilde{\Delta}(t) < 0 \ , \\ H(t-1) + \tilde{\Delta}(t) & \text{otherwise} \ , \end{cases} \tag{5}$$

where $\tilde{\Delta}$ is given by the equation:

$$\tilde{\Delta}(t) = \eta_{\text{in}} \Delta_+(t) - \eta_{\text{out}}^{-1} \Delta_-(t) \tag{6}$$

and $H(t_{\text{min}} - 1) = H_0$ is an initial value to be determined, t_{min} being the first hour of the time series. The storage works in the following way: Any excess power at any time is fed into the storage with an efficiency of η_{in}, unless the storage size is exceeded, in which case the storage is full. Any deficits in VRE power generation as compared to the load are covered by the storage with an efficiency of η_{out}, except if the storage runs empty, in which case the storage only provides partial coverage of the deficit. The dispatch strategy is illustrated in Figure 2.

To ensure *storage neutrality,* i.e. that the storage provides only as much energy as is stored, we determine H_0 in the following way: First, it is examined whether the generation can match the demand. This is the case if $\tilde{\Delta}$ sums up to a non-negative value, $\sum_t \tilde{\Delta}(t) \geq 0$ (equality is called *equilibrium*) or equivalently

$$\eta_{\text{in}} \eta_{\text{out}} \sum_t \Delta_+(t) \geq \sum_t \Delta_-(t) \ . \tag{7}$$

If this is the case, we set the temporary variable $H_{00} = C_S$, if not, $H_{00} = 0$. H_{00} is then used as an initial guess for H_0, and the final storage filling level

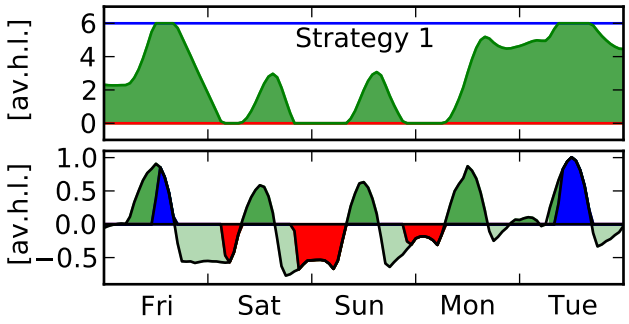

Figure 2: Top panel shows excerpt of a storage filling level time series resulting from applying the simple dispatch strategy. Lower panel shows excerpt of mismatch (outer black line) for the time series leading to the storage filling level time series in the top panel, as well as charge (dark green), discharge (light green), excess (blue) and balancing power (red), respectively. The excerpt of the time series shown is the time period 10–15 March 2000.

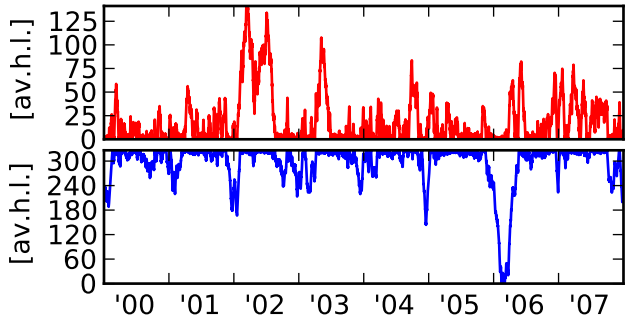

Figure 3: Top panel shows as an example the storage filling level time series resulting from $\gamma = 0.9$ and $\alpha_W = 0.6$ with a lossless, unconstrained storage. As $\gamma < 1$, the time series tends to be close 0. C_S^{eff} corresponds to the highest peak. Lower panel similarly shows the storage filling level time series resulting from $\gamma = 1.1$ and $\alpha = 0.6$. As $\gamma > 1$, the time series tends to be close to C_S^{eff}, which in turn is determined by the largest dip.

time series value $H(t_{\max})$, $t_{\max}$ being the last hour of the time series, is found. We then choose $H_0 = H(t_{\max})$. With this choice, the storage becomes neutral, which means that the storage does not contribute to the balancing, nor does it consume extra energy over the eight-year time span considered.

In case the whole storage range is not used, the storage filling level time series is shifted down so that the minimal value of the storage filling level becomes

0. For a lossless storage ($\eta_{\rm in} = \eta_{\rm out} = 1$), this happens if the storage is large enough to avoid additional average balancing. The effectively used storage size $C_S^{\rm eff}$ is then given by $\max_t H(t)$. By choosing C_S sufficiently large, making the storage size in practice unconstrained, the algorithm can in this way be used to determine the smallest storage size with the property that enlarging the storage size has no effect on what can be stored or dispatched. Assuming lossless storage with $\eta_{\rm in} = \eta_{\rm out} = 1.00$, the model with unconstrained storage size amounts to storing all excess for $\gamma \leq 1$, and exactly what is required to cover deficits for $\gamma \geq 1$. Figure 3 illustrates the storage filling level time series for unconstrained storage sizes.

2.5. Reduced mismatch time series

So far, we have defined the generation and load time series, the mismatch time series, the balancing time series and (additional) average balancing energy as well as the storage filling level time series. To model the interaction of the mismatch with the storage, we define a *reduced mismatch time series*, from which we can determine how storage affects balancing needs.

The changes in the filling level of the storage can be described by the time series $F(t)$ given by:

$$F(t) = H(t) - H(t-1) \ , \qquad t \geq t_{\rm min} \ . \tag{8}$$

Correspondingly, the power flow in and out of the storage is

$$\tilde{F}(t) = \eta_{\rm in}^{-1} F_+(t) - \eta_{\rm out} F_-(t) \ , \tag{9}$$

where positive values indicate that power flows in and negative values indicate that power flows out of the storage. We can now write the mismatch after storage transactions as

$$\Delta^{\rm r}(t) = \Delta(t) - \tilde{F}(t) \ , \tag{10}$$

where "r" stands for "reduced." The flows as well as the reduced mismatch is illustrated in Figure 2 for a lossless storage. The reduced mismatch is now

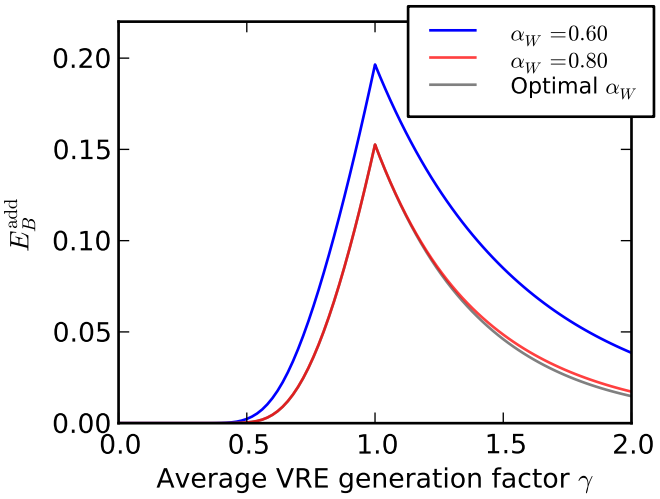

Figure 4: Additional average balancing E_B^{add} vs. average VRE generation factor γ without storage for $\alpha_W = 0.60$ (blue), $\alpha_W = 0.80$ (red) and the γ dependent optimal α_W (gray).

used to find the balancing time series for scenarios with combined storage and balancing, simply by

$$B(t) = \Delta^{\mathrm{r}}_{-}(t) \; . \tag{11}$$

This definition replaces the previous definition (3) of the balancing time series. It coincides with (3) when $C_S = 0$. The definitions of E_B and E_B^{add} are unchanged.

A case of more than one storage, e.g. a small high-efficient short-term and a larger low-efficient seasonal storage, can be modeled by feeding the reduced mismatch time series resulting from the application of the smaller storage to the model of the larger storage (see Sections 5 and 6).

3. The no storage and no additional average balancing scenarios

3.1. The no-storage scenario

Heide et al. (2011) has shown that in a scenario without storage and with $\gamma \geq 1$ the balancing needs are significant, even when the average VRE generation exceeds the load, and when aggregated over all of Europe. With the improved model presented here, we extend this scenario to the regime $\gamma < 1$.

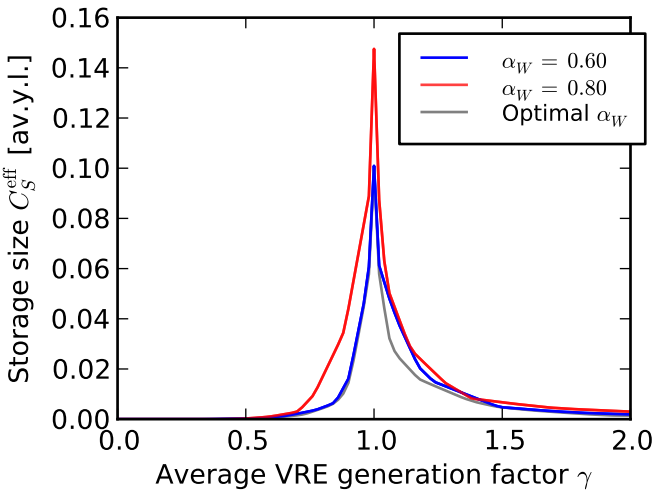

Figure 5: Storage singularity: Required storage size C_S^{eff} without additional average balancing vs. average VRE power generation factor γ for $\alpha_W = 0.60$ (blue), $\alpha_W = 0.80$ and the γ-dependent optimal α_W (gray).

As revealed in Figure 4 the integration of wind and solar power works well up to around $\gamma = 0.5$. Almost no additional average balancing is required up to this penetration. Above this limit large amounts of additional average balancing are required. Some of the generated power is potentially lost as excess generation, if it is not stored or if a new use for highly intermittent power is not found. The additional average balancing fraction E_B^{add} strongly peaks at $\gamma = 1$. The size of the peak strongly depends on the mix α_W. For $\alpha_W = 0.8$ it becomes a minimum. Also for $\gamma \neq 1$ the mix $\alpha_W = 0.8$ remains close to optimal. The optimal α_W minimizes balancing energy when no storage is present, cf. Heide et al. (2011), and turns out to be γ dependent. The numerical value of the optimal mix changes from 0.82 at $\gamma = 0.5$ via 0.80 at $\gamma = 1.00$ to 0.88 at $\gamma = 2.00$.

3.2. The no additional average balancing scenario

As already explored for $\gamma \geq 1$ in Heide et al. (2010, 2011), the alternative scenario where additional average balancing is completely avoided by storing

enough excess generation to cover additional average balancing needs, leads to very large storage sizes. Using the extended model, we can also cover $\gamma < 1$. At equilibrium ($\sum_t \tilde{\Delta}(t) = 0$), which for lossless storages is reached at $\gamma = 1.00$, a pronounced cusp singularity of required storage size appears. See Figure 5.

The choices of mix in Figure 5 reflect the findings of Heide et al. (2010, 2011), with the mix $\alpha_W = 0.60$ minimizing storage at $\gamma = 1.00$ and the mix $\alpha_W = 0.80$ minimizing balancing at $\gamma = 1.00$. Here, the optimal α_W is the γ dependent choice that minimizes the storage size without introducing additional average balancing. This optimal mix varies between 0.55 and 0.78 and is different from the optimal mix discussed in the previous subsection.

As seen in the figure, also for $\gamma < 1$ the storage size resulting from the mix $\alpha_W = 0.60$ is very close to the result for the optimal mix, and significantly better than that of the mix $\alpha_W = 0.80$. When γ gets larger than 1, the $\alpha_W = 0.60$ and $\alpha_W = 0.80$ cases quickly get very close to each other, reflecting the fact that, as excess generation increases, it is easier to keep the storage filled up and deficits become more rare, regardless of the mix. The case of optimal mix, however, performs slightly better in the γ range 1.00–1.50.

4. Combined usage of lossless storage and balancing

In this section, we investigate the advantages of combining storage and balancing. The scenarios described in Section 3 are extreme cases of a more general setup where storage and balancing are used in combination. In between the extremal balancing and storage scenarios, there is an unlimited number of possible combined balancing and storage strategies. In this paper, we will restrict ourselves to storage first strategies, with an imposed limit on the storage size, and balancing handling any remaining mismatch as described in Section 2. This class of strategies can be parametrized by the given storage size. They include the extremal balancing and storage scenarios as special cases by setting the imposed storage size limit to 0 or sufficiently large, respectively. A key property of the storage first strategies is that they minimize the additional average bal-

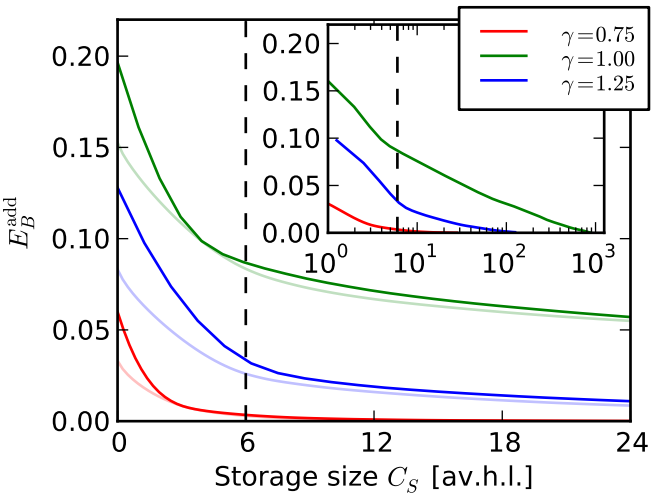

Figure 6: Additional average balancing fraction E_B^{add} as a function of small storage size C_S (shown on a linear scale). The darker curves are for $\alpha_W = 0.60$ and $\gamma = 0.75$ (red), 1.00 (green), 1.25 (blue). The light curves are obtained with an optimal mix which minimizes the additional average balancing fraction (see Figure 7). The inset shows E_B^{add} as a function of large storage sizes C_S (now shown on a log–scale). Note, that the endpoints of the curves reflect the findings of Figures 4 and 5.

ancing fraction for a given storage size. See Appendix A for a brief discussion of these and other strategies.

Figure 6 shows the relation between storage size and additional average balancing fraction. The figure shows three groups of curves. The red ($\gamma = 0.75$), green ($\gamma = 1.00$) and blue ($\gamma = 1.25$) are for the mix $\alpha_W = 0.60$. The respective light-coloured curves are obtained with an optimal mix, which minimizes E_B^{add} for a given storage size C_S and which differs slightly from $\alpha_W = 0.60$, especially for very small storage sizes C_S; see also Figure 7. As can be seen, all six curves $E_B^{\mathrm{add}}(C_S)$ are strongly convex, meaning that the reduction in balancing per unit of extra storage is much greater at the outset than for subsequent extensions of the storage size. There is a huge decrease in additional average balancing fraction for rather small storage sizes up to 6 av.h.l. (a quarter of a day). Beyond 6 av.h.l. of storage size the decrease of additional average balancing fraction is slow.

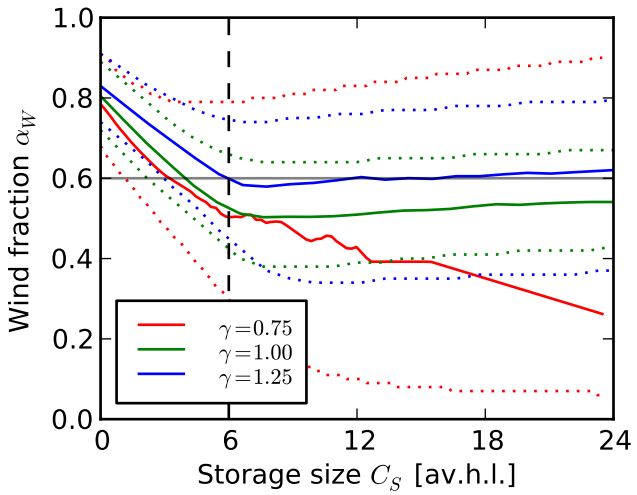

Figure 7: Optimal mix as a function of storage size for $\gamma = 0.75$ (red), 1.00 (green), 1.25 (blue). The respective dotted curves represent the upper and lower limits of α_W, which are obtained by allowing the additional average balancing fraction to be one percentage point larger than the minimized E_B^{add}. For comparison the choice $\alpha_W = 0.60$ is indicated by a gray line.

The different behavior of the additional average balancing fraction in the two regimes with storage size below and above 6 av.h.l. is easily explained. Caused by the solar power generation and the load, the mismatch (1) shows a pronounced diurnal pattern. For not too large mixes α_W the mismatch is mostly positive during day-light hours and negative during the night. A 6 av.h.l. storage is able to smooth this intraday cycle. It stores the positive mismatches occurring during the day and serves the negative mismatches occurring during the night; see also Heide et al. (2011). This explains the fast decrease of the excess balancing fraction with the introduction of a small storage size. How good the 6-hour storage is at smoothing the intraday cycle clearly depends on how much solar power is assumed to be in the system. If the solar share is very large, the 6 hours become inadequate and should be increased to about 12 hours in the extreme case $\alpha_W = 0$. Besides the diurnal time scale, the mismatch fluctuations are also influenced by the larger synoptic and seasonal time scales. The latter two cause the slow decrease of the additional average

balancing fraction for storage sizes beyond 6 av.h.l.

Note that the optimal mix between wind and solar power generation is also different for the two storage regimes (cf. Figure 7). Sufficiently below the 6 av.h.l. storage size, the optimal mix is $\alpha_W \simeq 0.8$, and the balancing energy increases relatively rapidly, as one deviates from the optimum value, as indicated by the dotted lines in Figure 7. This is a consequence mostly of the fact that the strong diurnal patterns of solar power makes it difficult to integrate large quantities of it into the power system without storage. At 6 av.h.l. the optimal mix has decreased to $\alpha_W = 0.5 - 0.6$ and the range of mixes that result in approximately the same balancing has increased significantly. For larger storage sizes the mix 0.6 results in a balancing energy close to the optimal mix for all γ's. In this regime the optimal mix is no longer sensitive to fluctuations on the diurnal time scale. It is dominated by the fluctuations occurring on the seasonal time scale. We note that the optimal mix $\alpha_W = 0.60$ differs from what is indicated in Schaber et al. (2012b) where a mix of 0.80 is suggested to be optimal in the presence of storage and a large VRE penetration.[6] As the $\alpha_W = 0.60$ curves are good approximators of the optimal mix curves for storages larger than 6 av.h.l., we will focus on this choice in what follows.

5. A lossless 6-hour storage with unconstrained balancing and seasonal storage

As described above, the introduction of a 6-hour storage has a significant impact on the required balancing energy as compared to no storage. Contrary to the enormous storage sizes needed in the full storage scenario (cf. Fig. 5), a 6-hour storage also appears to be technically feasible. Storages of that order may be realized by a combination of many different storage and time-shift

[6] This due to the fact that the measure used in Schaber et al. (2012b), which can be defined as $D = \sum_t |\Delta(t)|$, has no temporal memory. This means that, in principle, the storage could be full all summer and empty all winter, resulting in 1 yearly storage cycle, and still result in a small D.

technologies such as pumped hydro, compressed air, superconducting magnetic energy storages, different battery technologies, flywheels, capacitors (Beaudin et al. (2010)) and demand side management and smart grid (Strbac (2008)).

Figure 8a plots the additional average balancing fraction vs. average VRE generation factor for the mix $\alpha_W = 0.60$. The black curve is with a lossless 6-hour storage while the gray curve is without storage. The additional average balancing fraction is more than halved at $\gamma = 1.00$, where the difference is smallest in relative terms. For other values of γ the relative reduction in additional average balancing is larger. Whereas without storage significant amounts of additional average balancing appear beyond γ around 50%, this threshold is pushed to 75% when introducing the 6-hour storage. As for the other end of the range, where 3.9% of additional average balancing is needed at $\gamma = 2.00$, this is reduced to just 0.1% with a 6-hour storage.

Another option is to have two layers of storage: the high-efficient 6-hour storage and a low-efficient bulk seasonal storage. Additional storages with sizes far beyond 6 av.h.l. require high energy densities. An option could be hydrogen storage (Hedegaard and Meibom (2012); Beaudin et al. (2010); Kruse et al. (2002)). We first compute the reduced mismatch time series after applying the 6-hour storage to the generation–load mismatch time series, and the lower efficiency storage is then applied to this reduced mismatch time series. Since all that can be covered by the 6-hour storage is assumed to be lossless, we increase the overall energy efficiency by applying this first. This can be directly observed in Figure 8b, where the size for the less efficient hydrogen storage is shown as a function of γ with and without the 6-hour lossless storage for the mix $\alpha_W = 0.60$. Without the 6-hour storage, the size of the bulk hydrogen storage reaches equilibrium ($\sum_t \tilde{\Delta}(t) = 0$, see Section 2.4) at the peak $\gamma = 1.23$. The 6-hour storage lowers this value down to $\gamma = 1.10$ (here the equilibrium is at $\sum_t \tilde{\Delta}^{\mathrm{r}}(t) = 0$).

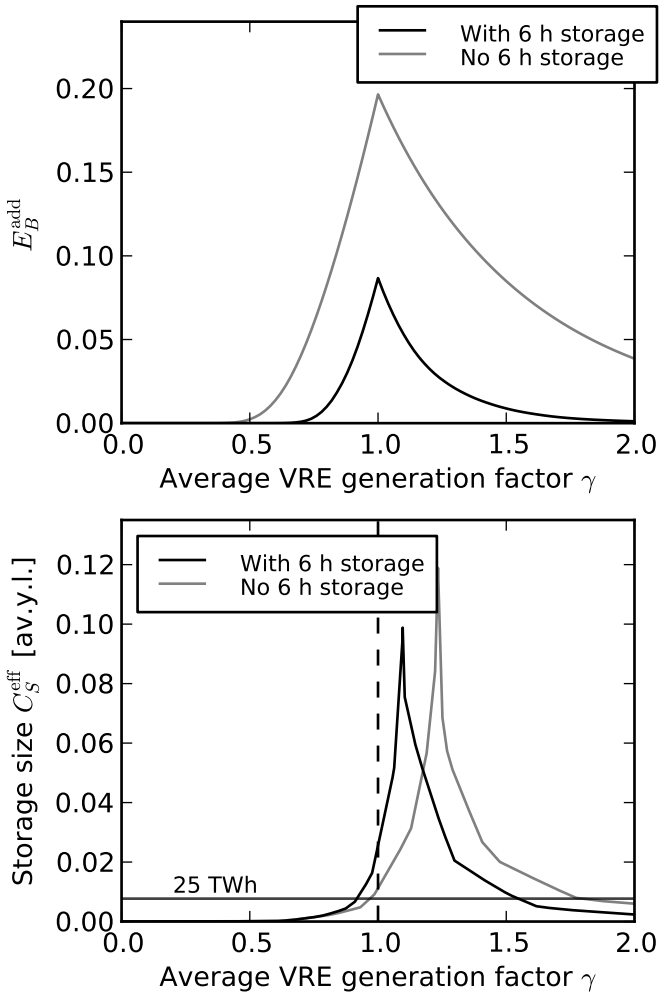

Figure 8: (a) additional average balancing fraction E_B^{add} and (b) storage size C_S^{eff} for a hydrogen storage vs. average VRE power generation factor γ with (black) and without (gray) first using a 6-hour lossless storage for $\alpha_W = 0.60$.

6. A lossless 6-hour storage with constrained hydro balancing and hydrogen storage

A possible way of providing a renewable form of balancing that can be dispatched on demand is to use the hydro power storage lakes of northern Scandinavia, the Alps and elsewhere in Europe. In France, Italy, Spain and

Switzerland alone, the current generation from storage lake facilities amounts to about 70 TWh/yr, and the total hydro power generation of Norway and Sweden amounts to 190 TWh/yr, most of which is generated from storage lake facilities (Lehner et al. (2005)). Here, we assume that at least 150 TWh/yr of the total European hydro power generation can be dispatched on demand. This amounts to about 5% of the average load, and to the best of our knowledge, it represents a conservative estimate. As an alternative to hydro power, other sources of dispatchable renewable balancing such as biomass fired power plants could also be assumed without changing the conclusions of the analysis.

Bulk seasonal storage in a fully renewable pan-European power system could be realized as e.g. underground hydrogen storage. Of the different types of underground storage types presently used for natural gas, only solution mined salt caverns are directly usable for hydrogen storage (Stone et al. (2009)). In Europe most of the suitable geological formations are located in northern Germany, and the combined working gas volume of all existing European facilities allows for storage of 32.5 TWh in the form of hydrogen (Gilhaus (2007)). In the following we assume that a total storage size of 25 TWh are made available for hydrogen storage and we use conversion efficiencies of $\eta_{\text{in}} = \eta_{\text{out}} = 0.60$.

With a total balancing energy of 150 TWh/yr and a 25 TWh hydrogen storage, as described above, we model the optimal combined operation with and without an additional lossless 6-hour storage (2.2 TWh). As outlined at the end of Section 2, first the high-efficient 6-hour storage, if included, is applied to the mismatch time series, next the reduced mismatch time series is confronted with the constrained hydrogen storage, and finally, the still existing (doubly reduced) mismatch determines the balancing needs. According to Figure 8b, for the mix $\alpha_W = 0.60$ the storage size of 25 TWh (corresponding to 0.008 av.y.l. in 2007-units) only represents a constraint for average VRE power generation factors γ between 0.97 and 1.80 without a 6-hour storage and between 0.92 and 1.55 with a 6-hour storage.

Now the question is which combinations of γ and α_W satisfy the 150 TWh/yr constraint of hydro balancing. The answer to this question is given in Figure 9

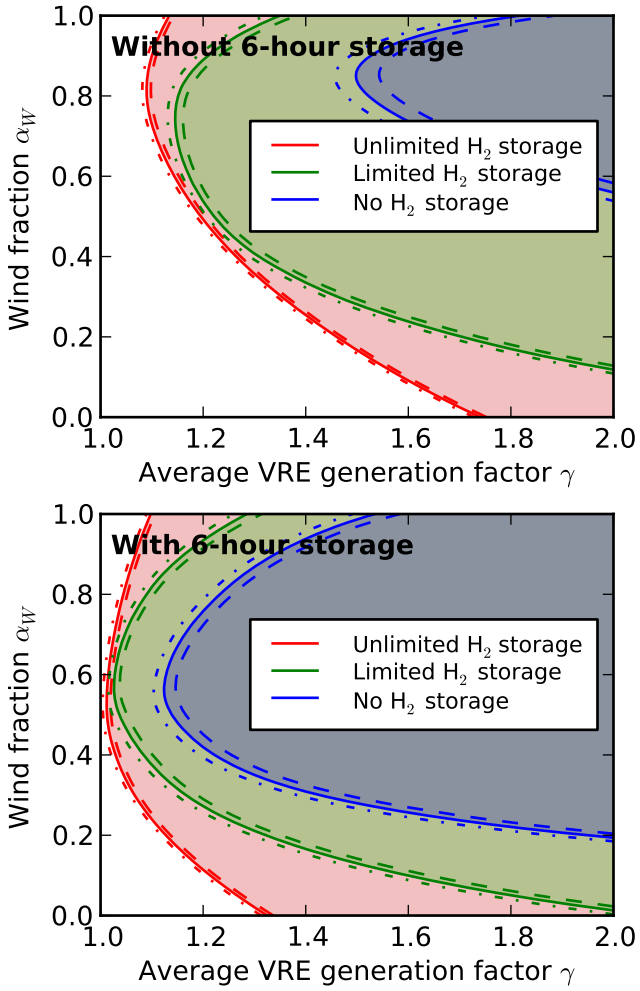

Figure 9: Contour plots indicating which γ–α_W combinations lead to a balancing need equal to 150 TWh/yr for the three scenarios (blue) no, (green) constrained (with 25 TWh) and (red) unconstrained (with effectively unlimited size) hydrogen storage. The top and bottom panels are respectively without and with a 6-hour lossless storage applied first. On both panels, the solid lines indicate where 150 TWh/yr balancing suffice, and the dash-dotted and dashed lines indicate the corresponding lines for 150 TWh/yr$\pm$10%, respectively.

for the six scenarios: no, constrained (25 TWh) and unconstrained hydrogen storage, combined with and without a lossless 6-hour storage. The figure shows the penetration levels and mixes that qualify as fully renewable. We note that a

scenario cannot qualify if the combined renewable power generation from wind, solar PV and hydro balancing does not equal or exceed the load on average. In the case studied here, hydro balancing corresponds to 0.046 av.h.l. so the minimum γ is 0.954 av.h.l. However, because some energy is lost when it is stored as hydrogen, and some wind and solar PV is curtailed, the actual minimum value of γ is higher.

Figure 9a shows the results of calculations without the lossless 6-hour storage. When none of the storages are present, the optimal mix is $\alpha_W = 0.85$ and the minimum value of γ is 1.50. The resulting average total renewable generation is about 1.55 av.h.l. since hydro balancing must be added to generation from wind and solar PV. In this scenario, the entire 0.55 av.h.l. is lost to curtailment. Adding the constrained 25 TWh hydrogen storage alone reduces the minimum value of γ to 1.15, now with $\alpha_W = 0.74$. An unconstrained hydrogen storage could reduce the value of γ further to 1.09 at an α_W of 0.81. In the two scenarios with either constrained or unlimited hydrogen storage, the overproduction is lost to a combination of storage conversion losses and curtailment.

Figure 9b shows how the three scenarios, described above, change when a lossless 6-hour storage (2.2 TWh) is added to the system. Now, a scenario without hydrogen storage can be made fully renewable at a γ of 1.12 and an $\alpha_W = 0.56$ mix. Thus, the impact of a lossless 6-hour storage is comparable to that of a 25 TWh hydrogen storage, albeit at a very different mix. When a 25 TWh hydrogen storage is added too, the optimal mix becomes $\alpha_W = 0.56$, and we find that $\gamma = 1.03$ suffice. In this case, increasing the hydrogen storage size beyond 25 TWh only has a marginal effect.

In the scenario where a 6-hour storage is added to the constrained hydrogen storage, the total storage size is increased from 25 to 27.2 TWh. However, only a small part of the reduction in γ from 1.15 to 1.03 can be attributed to this increase. Instead, the more important reasons for the decrease are: i) a higher total energy efficiency, where the lossless 6-hour storage allows efficient smoothing of the intra-day variations in the mismatch, and ii) it enables more efficient use of solar PV and, thus, a seasonal optimal mix between wind and

solar PV can be better utilized. As a result, the scenario which includes both the constrained hydrogen storage and the lossless 6-hour storage results in a combined average generation that corresponds to only $(3+5)\% = 8\%$ more than the average demand. Thus, this scenario has a high over-all energy efficiency and a low amount of overinstallation is needed. As such it is an example of a fully renewable European electricity supply based on wind, solar PV and a conservative estimate of hydro power generation alone.

7. Discussion and conclusion

We have investigated the ability of the power system to integrate any level of wind and solar power in a fully interconnected European power system. In our analysis, we have focused on the ability of both short-term and seasonal storage systems to increase the integrability. Our study addresses how the introduction of a certain amount of storage influences (1) the balancing energy needs and (2) the optimal generation mix. The analysis is based on high-resolution hourly weather data and electricity load for 27 European countries over the eight-year period 2000–2007.

Without additional balancing, a very pronounced cusp singularity of the needed storage size appears, peaking where the system is fully renewable (cf. Figure 5 and 8b). This is due to the fact that the storage filling level time series changes from being almost empty most of the time to being almost full most of the time, resembling a phase-transition. At its peak, the storage size amounts to at least 320 TWh or 10% of the annual load. For hydrogen storage and with suboptimal mix, the figure is higher. The technical implementation and physical location of such a storage is severely limited and may not be feasible (Heide et al. (2010)). With additional balancing, the need for such a large storage can, however, be avoided.

For storages of limited size, we have identified that a storage capable of storing 6 hours of average consumption – a quarter of an average day – is enough to remove the largest impact of the intraday mismatch, and thus significantly

reduce the balancing energy needs (cf. Figure 8). This implies that the optimal mix is shifted towards the seasonal optimal mix. A high-efficiency 6-hour storage more than halves the balancing energy needs at $\gamma = 1.00$ for a mix of $\alpha_W = 0.60$. The impact is even greater for both higher and lower penetration levels, allowing for full integration up to an average combined wind and solar power generation of about 75% (cf. Figure 8a). Without the 6-hour storage, this full integration can only be achieved up to about 50% for a fully connected Europe. As indicated in Figure 9, the impact of a 6-hour lossless storage (at optimal mix) is under certain circumstances almost as good as an unlimited hydrogen storage (at optimal mix). As opposed to the 320 TWh storage described above, a 6-hour storage, which corresponds to 2.2 TWh, can be realized by combining many different technological solutions including physical storages and time-shift technologies. Our results indicate that political support for the development of such technologies will be very beneficial for the system when the VRE penetration reaches 50% and will continue to have a great impact even in the fully renewable regime.

A seasonal storage can most likely only be realized with a low round-trip efficiency. A low-efficiency storage with a round-trip efficiency of 0.36 (0.60 each direction) and a storage size of 25 TWh (capable of providing up to $0.60 \cdot 25$ TWh $= 15$ TWh of stored energy), is technically realizable e.g. as hydrogen stored in solution mined salt caverns in northern Germany. In this scenario, the high-efficiency 6-hour storage serves the purpose of reducing the conversion losses, making the 150 TWh/yr of balancing sufficient for a γ of just 1.03 at an $\alpha_W = 0.56$ mix (again, cf. Figure 9). Without the 6-hour storage, the corresponding number would be $\gamma = 1.15$ ($\alpha_W = 0.80$ mix). Two fully renewable scenarios can be realized with a lossless 6-hour storage: one with $\gamma = 1.03$ and a 25 TWh hydrogen storage and one with $\gamma = 1.12$ and no additional storage. Whether there should be a hydrogen storage depends on the price of the 25 TWh compared to the price of going from $\gamma = 1.03$ to $\gamma = 1.12$, be it measured in environmental impact, economical terms or otherwise. If a highly efficient short-term storage comparable to our 6-hour storage does not become feasible, the

impact of a hydrogen storage is much greater, as it reduces the needed γ from 1.52 to 1.15 or 1.09, depending on whether the storage is limited to 25 TWh or not.

In conclusion, we find a significant synergy between storage and balancing. In particular, the effect of a highly efficient short-term storage dramatically reduces the balancing energy needs and allows for efficient use of a mix close to the seasonal optimal mix of wind and solar power. However, the additional gain by increasing the storage size of such a storage further is limited. A seasonal storage will most likely have a low efficiency, but in combination with a highly efficient short-term storage, the efficiency of the combined storage system is increased. This reduces the needed amount of overproduction in a fully renewable scenario. With a balancing of only 150 TWh/yr, e.g. coming from biomass or hydro power, a highly efficient 6-hour storage and a 25 TWh hydrogen storage employed, we find that a fully renewable scenario can be realized with an average wind and solar power production of only 3% more than the average load. Increasing the hydrogen storage size further does not lower the needed amount of overproduction substantially, and increasing the figure to 12%, a hydrogen storage can be completely avoided.

At present, the intracontinental power grid is becoming a bottleneck for the integration of non-dispatchable renewables such as wind and solar power. We find that even with a perfect grid, a combined penetration of wind and solar power of about 50% will lead to the need for an energy storage in order to avoid large losses. Investment in an efficient (virtual or physical) storage able to store the average demand for 6 hours is very important as it bears large benefits. However, we find that building a storage large enough to handle all surplus generation at large penetrations is unfeasible. A moderately large storage provides almost the same benefits, in particular in combination with the highly efficient small storage.

Acknowledgements

We would like to thank Rolando A. Rodriguez for proofreading several earlier versions of this manuscript and the two anonymous referees for comments that markedly improved the quality of this final paper. The first author was supported by the Carlsberg Foundation during all stages of the work. The second author is supported by DONG Energy.

Aboumahboub, T., Schaber, K., Tzscheutschler, P., Hamacher, T., 2010. Optimal configuration of a renewable-based electricity supply sector. WSEAS Transactions on Power Systems 5, 120–129.

Beaudin, M., Zareipour, H., Schellenberglabe, A., Rosehart, W., 2010. Energy storage for mitigating the variability of renewable electricity sources: An updated review. Energy for Sustainable Development 14, 302–314.

Czisch, G., 2005. Szenarien zur zukünftigen Stromversorgung, kostenoptimierte Variationen zur Versorgung Europas und seiner Nachbarn mit Strom aus erneuerbaren Energien. Ph.D. thesis. Universität Kassel.

Czisch, G., Giebel, G., 2007. Realisable scenarios for a future electricity supply based 100% on renewable energies, in: Energy Solutions for Sustainable Development Proceedings Risø International Energy Conference, Risø National Library, Technical University of Denmark. pp. 186–195.

ECF, 2010. Roadmap 2050: A practical guide to a prosperous, low-carbon Europe. Report. European Climate Foundation.

Gilhaus, A., 2007. Natural Gas Storage in Salt Caverns – Present Status, Developments and Future Trends in Europe. Technical Conference Paper. Solution Mining Research Institute.

Hedegaard, K., Meibom, P., 2012. Wind power impacts and electricity storage – a time scale perspective. Renewable Energy 37, 318–324.

Heide, D., von Bremen, L., Greiner, M., Hoffmann, C., Speckmann, M., Bofinger, S., 2010. Seasonal optimal mix of wind and solar power in a future, highly renewable europe. Renewable Energy 35, 2483–2489.

Heide, D., Greiner, M., von Bremen, L., Hoffmann, C., 2011. Reduced storage and balancing needs in a fully renewable european power system with excess wind and solar power generation. Renewable Energy 36, 2515–2523.

Jacobson, M.Z., Delucchi, M.A., 2011. Providing all global energy with wind, water, and solar power, part I: Technologies, energy resources, quantities and areas of infrastructure, and materials. Energy Policy 39, 1154–1169.

Kempton, W., Pimenta, F.M., Veron, D.E., Colle, B.A., 2010. Electric power from offshore wind via synoptic scale interconnection. PNAS 107, 7240–7245.

Kruse, B., Grinna, S., Buch, C., 2002. Hydrogen – Status og muligheter. Technical Report 6. Bellona. (in English).

Lehner, B., Czisch, G., Vassolo, S., 2005. The impact of global change on the hydropower potential of Europe: A model based analysis. Energy Policy 33, 839–855.

Lund, H., Mathiesen, B.V., 2009. Energy system analysis of 100% renewable energy systems – The case of Denmark in years 2030 and 2050. Energy 34, 524–531.

Martinot, E., Dienst, C., Weiliang, L., Qimin, C., 2007. Renewable energy futures: Targets, scenarios, and pathways. Annual Review of Environment and Resources 32, 205–239.

Rodriguez, R., Andresen, G.B., Becker, S., Greiner, M., 2012. Transmission needs in a fully renewable pan-European electricity system, in: Uyar, T.S., Sağlam, M., Sulukan, E. (Eds.), 2nd International 100% Renewable Energy Conference and Exhibition (IRENEC 2012) Proceedings, Maltepe – Istanbul, Turkey. pp. 320–324.

Schaber, K., Steinke, F., Hamacher, T., 2012a. Transmission grid extensions for the integration of variable renewable energies in europe: Who benefits where? Energy Policy 43, 123–135.

Schaber, K., Steinke, F., Mühlich, P., Hamacher, T., 2012b. Parametric study of variable renewable energy integration in europe: Advantages and costs of transmission grid extensions. Energy Policy 42, 498–508.

Stone, H.B.J., Veldhuis, I., Richardson, R.N., 2009. Underground hydrogen storage in the UK. The Geological Society, London, Special Publications 313, 217–226.

Strbac, G., 2008. Demand side management: Benefits and challenges. Energy Policy 36.

Widén, J., 2011. Correlations between large-scale solar and wind power in a future scenario for Sweden. IEEE Transactions on Sustainable Energy 2, 177–184.

Yao, R., Steemers, K., 2005. A method of formulating energy load profile for domestic buildings in the UK. Energy and Buildings 37, 663–671.

Appendix A. Strategies

In this appendix, we discuss the optimality of the "storage first" strategy with regard to balancing minimization for a given storage size and give a few examples of other strategies with other optimality properties. The fact that the "storage first" strategy is indeed optimal with respect to minimizing balancing energy follows from a simple induction argument, which is left to the interested reader as an easy exercise for the mathematically trained.

We stress that this strategy is not the only optimal strategy in this respect. Recall that the presented storage first strategy acts on an hour-by-hour basis by using the storage to cover deficits in the generation–load mismatch time series if the storage is not empty, and balancing in case the storage is or runs empty, and

in case of a positive mismatch, the excess generation is put into the storage if the storage is not already full. This way of acting makes no use of forecasts. Assuming perfect forecast, however, the same action could be performed on larger time intervals, in our case same-sign intervals, i.e. we split the time series in the largest chunks of intervals where the mismatch time series does not change sign. Having done this, one can now check to see how much of the integral of a positive mismatch interval can fit into the storage and how much of the integral of a negative mismatch interval can be covered by what is in the storage. Depending on what one wants to reduce (excess, balancing, storage charge/discharge power quantiles), one can then either cover the negative mismatches by using the storage to cover the most negative part of the mismatch (trough filling) or by using the storage to cover with a more or less constant storage power output (top filling), and vice versa for the positive mismatches (peak shaving and bottom shaving, respectively). In either case, the energy sum of what is used or absorbed by the storage in any given same-sign interval remains the same as for the storage first strategy, leaving the minimization with respect to balancing energy unaffected. The original version (Strategy 1 – "storage first") and two combinations (peak shaving–trough filling (Strategy 2) and bottom shaving–top filling (Strategy 3), respectively) are illustrated in Figure A.10.

Applying these three strategies to the same mismatch time series clearly result in the same balancing energies, but the quantiles of the storage charge and discharge powers and balancing power differ significantly – in particular for large γ's. Even minor changes in the storage–balancing strategies can have significant impact on the storage charge and discharge powers and the balancing power quantiles, and hence the needed installed power capacities.

Another strategy, which we call Strategy 4, that leads to the same balancing energy but a reduced charge and discharge capacity is found by the following algorithm: First, Strategy 1 is applied to determine how low the balancing energy can get for the given C_S. Then the charge capacity is reduced until it results in a larger balancing energy as compared to the unconstrained charging capacity. Now the charge capacity is kept fixed at the least capacity that does

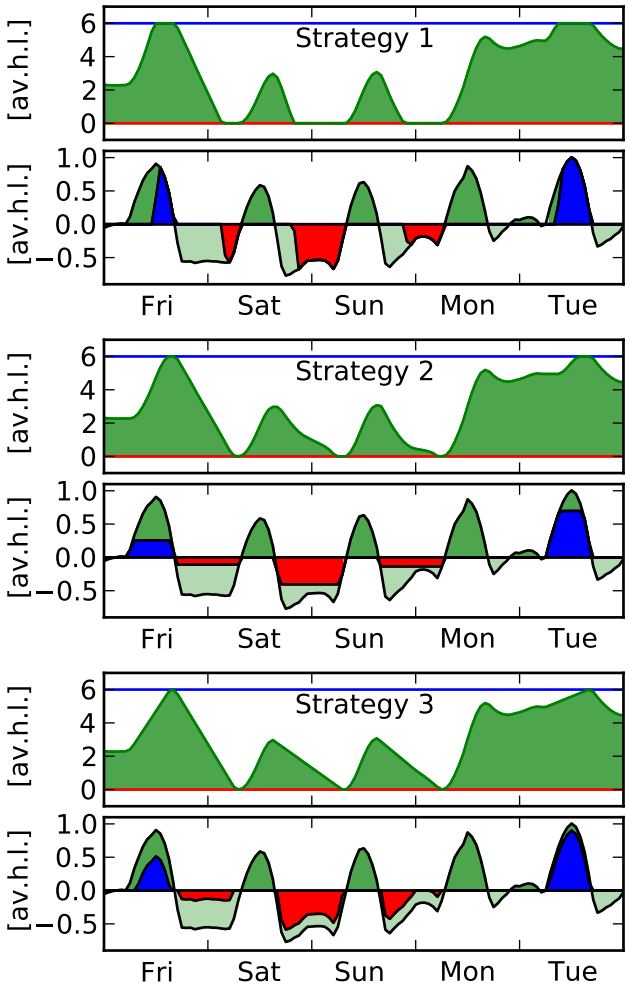

Figure A.10: Storage filling level (top panels) and mismatch, storage flow, excess and balancing power (bottom panels) for Strategies 1, 2 and 3, respectively. The positive mismatch is divided into a dark green and a blue part: Dark green is stored, while blue is excess power not absorbed by storage. Likewise, the negative mismatch is divided into a light green and a red part: Light green is covered by storage while the red represents coverage by balancing. The excerpt of the time series shown is the time period 10–15 March 2000.

not affect the balancing energy, while the discharge capacity is reduced until it results in larger balancing energy.

A suboptimal strategy along the same lines, Strategy 5, can be defined as

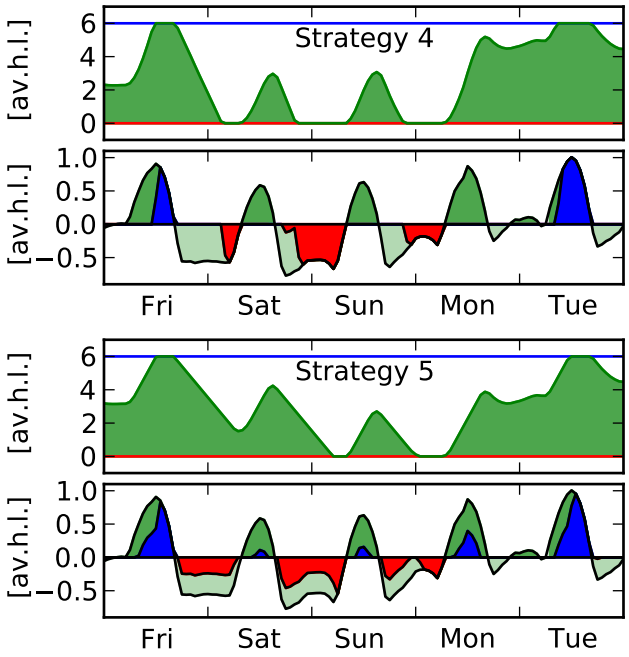

Figure A.11: Storage filling level (top panels) and mismatch, storage flow, excess and balancing power (bottom panels) for Strategies 4 and 5, respectively. See Figure A.10 for explanation of the color coding.

Strategy 4, but with the difference that a slightly higher balancing energy, say 10% larger, is allowed. Strategies 4 and 5 are illustrated in Figure A.11. In this concrete example, where the balancing energy is allowed to be 10% larger ($E_B = 0.1$ instead of $E_B = 0.09$) for Strategy 5, $\gamma = 1.0$ and $\alpha_W = 0.6$, the storage charge and discharge capacities are both approximately halved as compared to Strategy 4, and compared to the other strategies, the difference is even larger.

We will not pursue this issue any further in this paper, as a more complex model including transmission and storage sites seems to be needed in order to give useful results.